asymmetric unit (molecule B). Density for the other two molecules was broken and hard to interpret. The skeleton for molecule B was used to generate a molecular envelope for NCS averaging. Initial rotation matrices describing the relative orientations of molecules A, B and C were calculated from the heavy-atom sites (mercury bound to five sites in each of the three molecules). NCS averaging with DM[25] was used to improve phases at 2.7 Å resolution, and then extend phases to 2.2 Å, the limit of the native data set. The resulting electron density map was readily interpretable (Fig. 2). A model including residues 47–351 of each of the three molecules was built using the graphics program O[26]. No electron density is seen for 24 residues at the amino terminus. The model was refined using simulated annealing and positional refinement in X-PLOR[27], with tight NCS restraints. The model includes 669 water molecules, which were positioned by using the program ARP (V.Lamzin). An overall thermal B factor and tightly restrained individual B factors were refined, and a bulk-solvent model was incorporated. Crystallographic *R* values and stereochemical parameters are presented in Table 1.

The structure of the Cbl-N/ZAP70 phosphopeptide complex was determined by molecular replacement with the program AmoRe[28]. Use of the complete unliganded Cbl-N structure as a search model yielded clear rotation and translation peaks, and maps phased with the appropriately positioned model revealed strong electron density for the 4H and EF-hand domains, but no interpretable density for the SH2 domain. The model was therefore broken into two fragments (residues 47–265 and residues 266–351), and the rotation and translation searches were repeated with each fragment. The 4H/EF-hand fragment yielded a solution essentially identical to that from the intact model. The SH2 domain was then positioned using translation searches conducted in the context of the appropriately positioned 4H/EF-hand fragment. After rigid-body and positional refinement using X-PLOR[27], electron density maps calculated with the combined model revealed clear density for all domains, and readily interpretable density for the bound ZAP-70 phosphopeptide. After construction of the peptide, the structure was refined with iterative cycles of manual refitting and simulated annealing and positional refinement in X-PLOR (Table 1). Restrained individual temperature factors were refined. The model includes residues 47–351 of c-Cbl, residues 289–297 of ZAP-70, and 358 water molecules.

Illustrations

Figure 1a was prepared with MOLSCRIPT[29], Fig. 2 with program O[26], and Figs 1e and 3 with GRASP[30].

Received 7 December 1998; accepted 19 January 1999.

1. Thien, C. B. & Langdon, W. Y. c-Cbl: a regulator of T cell receptor-mediated signalling. *Immunol. Cell Biol.* **76,** 473–482 (1998).
2. Liu, Y. C. & Altman, A. Cbl: Complex formation and functional implications. *Cell Signal.* **10,** 377–385 (1998).
3. Miyake, S. *et al.* The Cbl proto-oncogene product: From enigmatic oncogene to center stage of signal transduction. *Crit. Rev. Oncogen.* **8,** 189–218 (1998).
4. Wange, R. L. & Samelson, L. E. Complex complexes: signaling at the TCR. *Immunity* **5,** 197–205 (1996).
5. Thien, C. B. & Langdon, W. Y. EGF receptor binding and transformation by v-*cbl* is ablated by the introduction of a loss-of-function mutation from the *Caenorhabditis elegans sli-1* gene. *Oncogene* **14,** 2239–2249 (1997).
6. Lupher, M. L. Jr, Songyang, Z., Shoelson, S. E., Cantley, L. C. & Band, H. The Cbl phosphotyrosine-binding domain selects a D(N/D)XpY motif and binds to the Tyr292 negative regulatory phosphorylation site of ZAP-70. *J. Biol. Chem.* **272,** 33140-33144 (1997).
7. Ikura, M. Calcium binding and conformational response in EF-hand proteins. *Trends Biochem. Sci.* **21,** 14–17 (1996).
8. Kuriyan, J. & Cowburn, D. Modular peptide recognition domains in eukaryotic signaling. *Annu. Rev. Biophys. Biomol. Struct.* **26,** 259–288 (1997).
9. Saurin, A. J., Borden, K. L., Boddy, M. N. & Freemont, P. S. Does this have a familiar RING? *Trends Biochem. Sci.* **21,** 208–214 (1996).
10. Blake, T. J., Shapiro, M., Morse, H. C. & Langdon, W. Y. The sequences of the human and mouse c-*cbl* proto-oncogenes show v-*cbl* was generated by a large truncation encompassing a proline-rich domain and a leucine zipper-like motif. *Oncogene* **6,** 653–657 (1991).
11. Galisteo, M. L., Dikic, I., Batzer, A. G., Langdon, W. Y. & Schlessinger, J. Tyrosine phosphorylation of the c-*cbl* proto-oncogene protein product and association with epidermal growth factor (EGF) receptor upon EGF stimulation. *J. Biol. Chem.* **270,** 20242–20245 (1995).
12. Deckert, M., Elly, C., Altman, A. & Liu, Y. C. Coordinated regulation of the tyrosine phosphorylation of Cbl by Fyn and Syk tyrosine kinases. *J. Biol. Chem.* **273,** 8867–8874 (1998).
13. Yoon, C. H., Lee, J., Jongeward, G. D. & Sternberg, P. W. Similarity of *sli-1*, a regulator of vulval development in *C. elegans*, to the mammalian proto-oncogene c-*cbl*. *Science* **269,** 1102–1105 (1995).
14. Meisner, H. et al. Interactions of *Drosophila* Cbl with epidermal growth factor receptors and role of Cbl in R7 photoreceptor cell development. *Mol. Cell Biol.* **17,** 2217–2225 (1997).
15. Ota, Y. & Samelson, L. E. The product of the proto-oncogene c-*cbl*: a negative regulator of the Syk tyrosine kinase. *Science* **276,** 418–420 (1997).
16. Holm, L. & Sander, C. Dali: a network tool for protein structure comparison. *Trends Biochem. Sci.* **20,** 478–480 (1995).
17. Kretsinger, R. H. EF-hands embrace. *Nature Struct. Biol.* **4,** 514–516 (1997).
18. Essen, L. O., Perisic, O., Cheung, R., Katan, M. & Williams, R. L. Crystal structure of a mammalian phosphoinositide-specific phospholipase Cδ. *Nature* **380,** 595–602 (1996).
19. de Beer, T., Carter, R. E., Lobel-Rice, K. E., Sorkin, A. & Overduin, M. Structure and Asn-Pro-Phe binding pocket of the Eps15 homology domain. *Science* **281,** 1357–1360 (1998).
20. Becker, S., Groner, B. & Muller, C. W. Three-dimensional structure of the Stat3β homodimer bound to DNA. *Nature* **394,** 145–151 (1998).
21. Chen, X. *et al.* Crystal structure of a tyrosine phosphorylated STAT-1 dimer bound to DNA. *Cell* **93,** 827–839 (1998).
22. Hatada, M. H. et al. Molecular basis for the interaction of the protein tyrosine kinase ZAP-70 with the T-cell receptor. *Nature* **377,** 32–38 (1995).
23. Eck, M. J., Shoelson, S. E. & Harrison, S. C. Recognition of a high-affinity phosphotyrosyl peptide by the Src homology-2 domain of p56^{lck}. *Nature* **362,** 87–91 (1993).
24. Otwinowski, Z. & Minor, W. Processing of X-ray diffraction data collected in oscillation mode. *Methods Enzymol.* **276,** 307–326 (1997).
25. Collaborative Computational Project Number 4. The CCP4 suite: Programs for protein crystallography. *Acta Crystallogr. D* **50,** 760–776 (1994).
26. Jones, T. A., Zhou, J. Y., Cowan, S. W. & Kjeldgaard, M. Improved methods for building protein models in electron density maps and the location of errors in these models. *Acta Crystallogr. A* **47,** 110–119 (1991).
27. Brunger, A. *X-PLOR Version 3.0: A System for Crystallography and NMR* (Yale University Press, New Haven, 1992).
28. Navaza, J. (ed.) *AMoRe: A New Package for Molecular Replacement* (SERC, Daresbury, UK, 1992).
29. Kraulis, P. J. MOLSCRIPT: a program to produce both detailed and schematic plots of protein structures. *J. Appl. Crystallogr.* **24,** 946-950 (1991).
30. Nicholls, A., Sharp, K. A. & Honig, B. Protein folding and association: insights from the interfacial and thermodynamic properties of hydrocarbons. *Proteins Struct. Funct. Genet.* **11,** 281-296 (1991).

Acknowledgements

We thank C. Dahl for synthesis and purification of the ZAP-70 phosphopeptide, the staff at MacCHESS for assistance with data collection, and S. Harrison and T. Roberts for comments on the manuscript. M.J.E. is a recipient of a Burroughs–Wellcome Career Award in the Biomedical Sciences. Diffraction data were recorded at the Cornell High Energy Synchrotron Source (CHESS), which is supported by grants from the NSF and NIH.

Correspondence and requests for materials should be addressed to M.J.E. (e-mail: eck@red.dfci.harvard.edu). Atomic coordinates have been deposited with the Protein Data Bank (Brookhaven National Laboratory) under accession numbers 2cbl and 1b47.

Nature **401,** 708–712; 1999

Two subsets of memory T lymphocytes with distinct homing potentials and effector functions

Federica Sallusto*, Danielle Lenig*, Reinhold Förster†, Martin Lipp† & Antonio Lanzavecchia*

** Basel Institute for Immunology, Grenzacherstrasse 487, Postfach, CH-4005 Basel, Switzerland*
† Max-Delbrueck-Center for Molecular Medicine, Robert Rossle Strasse 10, 13122 Berlin-Buch, Germany

Naive T lymphocytes travel to T-cell areas of secondary lymphoid organs in search of antigen presented by dendritic cells[1,2]. Once activated, they proliferate vigorously, generating effector cells that can migrate to B-cell areas or to inflamed tissues[3–6]. A fraction of primed T lymphocytes persists as circulating memory cells that can confer protection and give, upon secondary challenge, a qualitatively different and quantitatively enhanced response[7–9]. The nature of the cells that mediate the different facets of immunological memory remains unresolved. Here we show that expression of CCR7, a chemokine receptor that controls homing to secondary lymphoid organs, divides human memory T cells into two functionally distinct subsets. CCR7$^-$ memory cells express receptors for migration to inflamed tissues and display immediate effector function. In contrast, CCR7$^+$ memory cells express lymph-node homing receptors and lack immediate effector function, but efficiently stimulate dendritic cells and differentiate into CCR7$^-$ effector cells upon secondary stimulation. The CCR7$^+$ and CCR7$^-$ T cells, which we have named central memory (T_{CM}) and effector memory (T_{EM}), differentiate in a step-wise fashion from naive T cells, persist for years after immunization and allow a division of labour in the memory response.

When blood-borne naive T cells home to lymph nodes, they first roll on high endothelial venules using CD62L. This allows the chemokine receptor CCR7 to engage its ligand SLC, which is displayed by endothelial cells[10]. The CCR7–SLC interaction activates integrins that promote firm adhesion and transmigration of the T cells into the lymph node[11,12]. In contrast to naive T cells, memory/effector cells migrate mostly through peripheral tissues[13]. This migration mediates rapid protective responses and is controlled by the expression of different sets of integrins and chemokine receptors[1,14]. However, some memory T cells must also reach the lymph nodes to mount secondary proliferative responses. We considered whether the two facets of the memory response might depend on subsets of memory T cells invested with distinct homing and effector capacities.

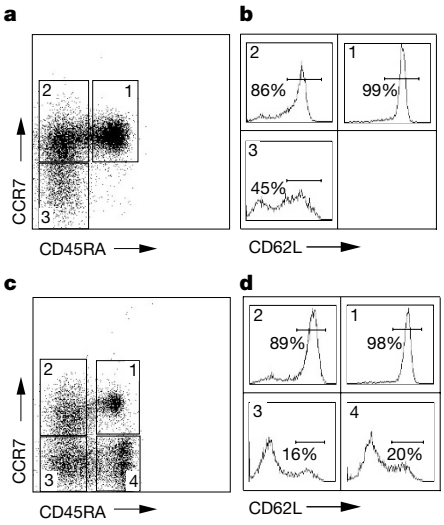

Figure 1 CCR7 and CD62L are co-expressed on a subset of peripheral blood memory CD4$^+$ and CD8$^+$ T cells. CD4$^+$ (**a**, **b**) and CD8$^+$ (**c**, **d**) lymphocytes were stained with monoclonal antibodies to CD45RA and CCR7, which identified three and four subsets, respectively. These subsets were sorted and analysed for the expression of CD62L, and the percentage of bright cells is indicated (**b**, **d**). Upon serial analysis, the proportion of cells in the different compartments was rather stable in the same individual, but more variable among individuals, the variability being more pronounced in the CD8 than in the CD4 compartment. Comparable results were obtained using two anti-CCR7 antibodies (clones 3D12 and 10H5).

Because CCR7 and CD62L are essential for lymphocyte migration to lymph nodes[1,15], the co-expression of these receptors might distinguish a putative subset of memory T cells that home to lymph nodes. Human naive and memory T cells can be identified by the reciprocal expression of the CD45RA or CD45R0 isoforms[16]. Staining of peripheral blood T cells with antibodies to CD45RA and CCR7 revealed three subsets of CD4$^+$ cells: one naive CD45RA$^+$CCR7$^+$; and two memory subsets, CD45RA$^-$CCR7$^+$ and CD45RA$^-$CCR7$^-$ (Fig. 1a). Both naive and CCR7$^+$ memory cells expressed high levels of CD62L, whereas the CCR7$^-$ memory cells expressed CD62L to a lower and variable extent (Fig. 1b). Within CD8$^+$ T cells, the same three subsets could be identified, with an extra subset of CD45RA$^+$CCR7$^-$ cells (Fig. 1c). In addition, the two CCR7$^+$ subsets expressed high levels of CD62L, whereas most of the cells among the two CCR7$^-$ subsets lacked CD62L (Fig. 1d). This shows that lymph-node-homing receptors are expressed on a distinct subset of memory CD4 and CD8 T cells; furthermore, it identifies a subset of CD8$^+$ cells that is CD45RA$^+$, but that lacks both CCR7 and CD62L.

A number of chemokine receptors and adhesion molecules are involved in lymphocyte migration to secondary lymphoid organs or to tissues under homeostatic or inflammatory conditions[1,14]. CCR7$^-$ memory T cells express high levels of β1 and β2 integrins, which are required for homing to inflamed tissues[17], as well as tissue-specific homing receptors such as CD103 and CLA (Table 1). Receptors for inflammatory chemokines, such as CCR1, CCR3 and CCR5, which have been found on memory/effector cells[18,19], were selectively

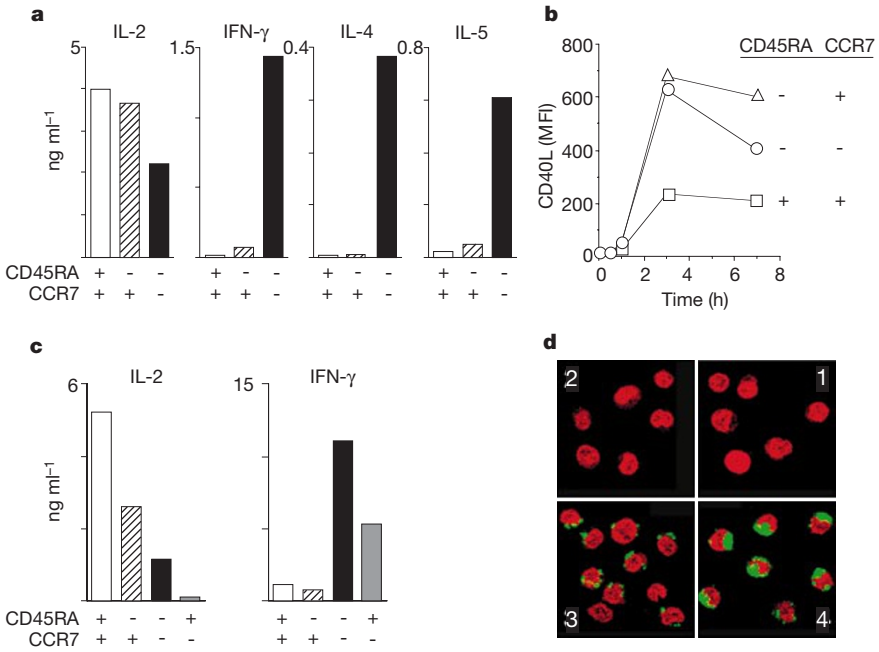

Figure 2 CCR7$^+$ and CCR7$^-$ memory T cells display different effector functions. **a**, **b**, The three subsets of CD4$^+$ T cells were sorted according to the expression of CCR7 and CD45RA as in Fig. 1 and tested for their capacity to produce IL-2, IFN-γ, IL-4 and IL-5 (**a**) and for the kinetics of surface CD40L upregulation (**b**) following polyclonal stimulation. **c**, **d**, The four subsets of CD8$^+$ T cells were sorted according to the expression of CCR7 and CD45RA as in Fig. 1 and tested for their capacity to produce IL-2 or IFN-γ (**c**) or were immediately stained with anti-perforin antibody (green) and counterstained with propidium iodide (red) (**d**). In the CD8$^+$ CD45RA$^+$ compartment, CCR7 expression allows us to discriminate naive cells (1) from effector cells (4) (ref. 26). Comparable results were obtained in 12 healthy donors.

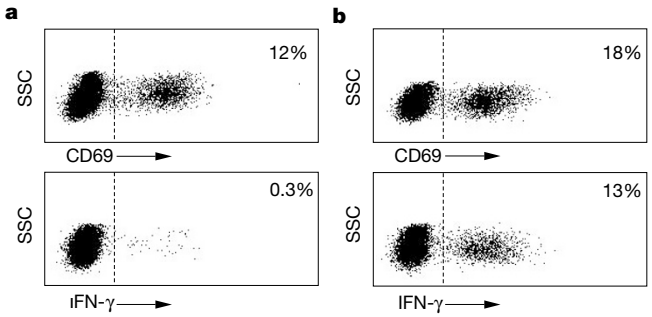

Figure 3 Rapid production of IFN-γ following stimulation of CCR7⁻ memory T cells. CD45RA⁻CCR7⁺ (**a**) and CD45RA⁻CCR7⁻ (**b**) CD4 T cells were stimulated for 7 h with autologous dendritic cells pulsed with 100 ng ml^{-1} TSST and stained with antibodies to CD69 and IFN-γ. CD69⁺ cells were less than 2% in unstimulated cultures.

expressed in the CCR7⁻ memory subset. On the other hand, CCR7⁺ memory cells had a distinct phenotype. They expressed intermediate levels of β1 and β2 integrins, as well as CCR4, CCR6 and CXCR3 on various proportions of cells. T-cell activation markers such as CD69 and CD25 were expressed only on a small fraction of the two memory subsets, whereas HLA-DR was expressed on about 10% of the CCR7⁻ memory cells. Together, these results imply that CCR7⁺ memory T cells share migratory routes with naive T cells, although the expression of additional receptors such as CCR4 may allow them to respond to a wider spectrum of chemokines and interact more effectively with dendritic cells[20,21].

Memory T cells carrying distinct homing receptors might participate in different types of immune responses and therefore might have different effector capacities. T-cell help for dentritic cells and B cells is dependent on expression of CD40L[22], whereas protective responses in the tissues are mediated by T cells that produce effector cytokines, such as interferon-γ (IFN-γ) or interleukin-4 (IL-4), or release stored perforin[23,24]. The naive and two memory CD4 subsets were sorted and compared for their capacity to produce cytokines and upregulate CD40L following stimulation. As shown in Fig. 2a, both naive T cells and CCR7⁺ memory cells produced IL-2 only. In contrast, the CCR7⁻ memory subset produced high levels of IL-4, IL-5 and IFN-γ and moderately reduced levels of IL-2. Upon activation, the extent of CD40L upregulation was comparable in the two memory subsets and was higher than in naive T cells; however, the kinetics of upregulation were comparable, indicating that, unlike tonsil T cells[25], circulating memory T cells do not contain stored CD40L (Fig. 2b). Rapid production of IFN-γ was detected in most CCR7⁻, but only a negligible fraction of CCR7⁺ memory cells following stimulation with autologous dendritic cells pulsed with a bacterial superantigen (Fig. 3). Within the four CD8⁺ T-cell subsets, IFN-γ production and perforin-containing granules were restricted to the CCR7⁻ cells (Fig. 2c, d). Perforin expression was particularly prominent in the CD45RA⁺CCR7⁻ population that corresponds to a reported population of terminally differentiated CD27⁻ effector T cells[26]. CD8⁺ cells progressively lost IL-2 production, presumably as a function of their differentiation from naive cells to effectors.

Table 1 Surface molecules on peripheral blood naive and memory CD4⁺ T-cell subsets

		CD45RA⁺ CCR7⁺	CD45RA⁻ CCR7⁺	CD45RA⁻ CCR7⁻
CD3	(%)	>99	>99	>99
CD69	(%)	<0.1	2	3
CD25	(%)	<0.1	4	8
HLA-DR	(%)	<0.1	1	12
CD18	(MFI)	38	49	75
CD11a	(MFI)	90	140	218
CD11b	(%)	<0.1	<0.1	35
CD29	(MFI)	0	10/36*	43
CD49d	(MFI)	10	19/2	33/2
CD49e	(%)	<0.1	<0.1	10
CLA	(%)	<0.1	4	25
CD103	(%)	<0.1	<0.1	1
CXCR4	(%)	98	22	11
CCR4	(%)	<0.1	18	6
CCR6	(%)	<0.1	40	45
CXCR3	(%)	<0.1	34	61
CCR1	(%)	<0.1	1	14
CCR3	(%)	<0.1	<0.1	4
CCR5	(%)	<0.1	2	52

Three subsets of peripheral blood CDE4⁺ cells were sorted by expression of CD45RA or CD45R0 and CCR7. The sorted cells were stained and analysed for the expression of adhesion moelcules and chemokine receptors. MFI, mean fluorescence intensity.
* Mean value of major and minor peak.

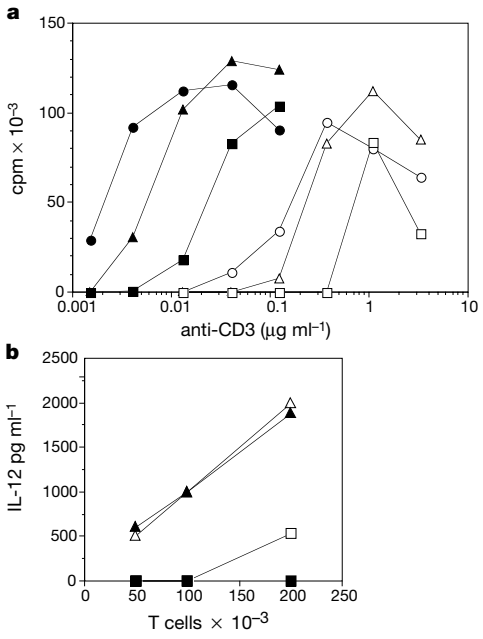

Figure 4 CCR7⁺ memory cells show enhanced responsiveness to T-cell receptor triggering and potently activate dendritic cells to produce IL-12. **a**, Proliferative response of naive T cells (squares), CCR7⁺ (triangles) and CCR7⁻ (circles) memory T cells to different concentrations of plastic-bound anti-CD3 monoclonal antibody in the absence (empty symbols) or in the presence (filled symbols) of anti-CD28. **b**, IL-12 p70 production by dendritic cells cultured with naive T cells (squares) or CCR7⁺ memory T cells (triangles). Dendritic cells were pulsed with toxic shock syndrome toxin (TSST) at 100 ng ml^{-1} (empty symbols) or 1 ng ml^{-1} (filled symbols). Both T-cell populations contained similar proportions of Vβ2⁺ cells.

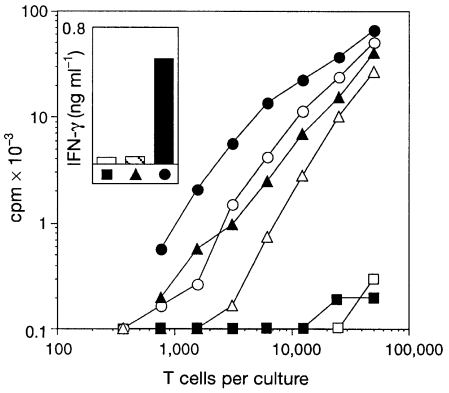

Figure 5 Proliferative responses to recall antigens can be detected in both CCR7$^+$ and CCR7$^-$ subsets but not in naive T cells. Proliferative response of CD45RA$^+$ CCR7$^+$ naive T cells (squares), CD45RA$^-$CCR7$^+$ (triangles) and CD45RA$^-$CCR7$^-$ memory T cells (circles) in response to tetanus toxoid presented by autologous monocytes. Responder cells from the same individual were tested 10 years after vaccination (empty symbols) and two weeks after a booster (filled symbols). Inset shows IFN-γ production in the 24-h culture supernatant using an input of memory cells giving comparable proliferative responses.

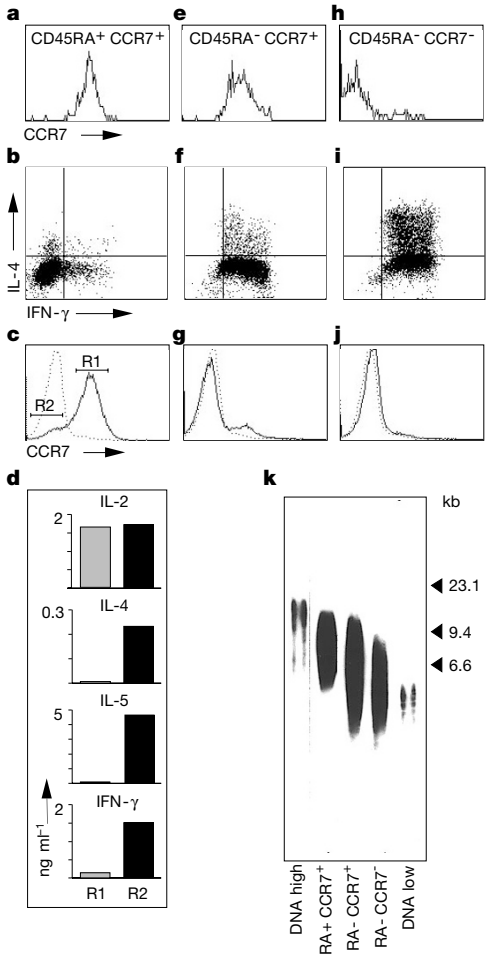

Figure 6 Differentiation potential of naive and memory T-cell subsets. **a**–**d**, Loss of CCR7 following *in vitro* stimulation of naive T cells correlates with acquisition of effector function. CD4$^+$ naive T cells (CD45RA$^+$, CCR7$^+$) were sorted from peripheral blood (**a**), stimulated with anti-CD3 + anti-CD28, expanded for 10 days in IL-2 and tested for their capacity to produce IFN-γ and IL-4 (**b**) or for CCR7 expression (**c**). CCR7$^+$ (R1) and CCR7$^-$ cells (R2) were sorted and immediately tested for their capacity to produce cytokines following polyclonal stimulation (**d**). **e**–**g**, Rapid polarization of CCR7$^+$ memory T cells following *in vitro* stimulation. CD4$^+$, CD45RA$^-$, CCR7$^+$ T cells were sorted from peripheral blood (**e**), stimulated, expanded and tested for cytokine production (**f**) and CCR7 expression (**g**). **h**–**j**, CD4$^+$, CD45RA$^-$, CCR7$^-$ T cells isolated and stimulated as above retained a stable effector phenotype. **k**, Length of telomeres in peripheral blood naive and memory CD4$^+$ T-cell subsets. kb, kilobases.

We then examined the activation requirements, which are less stringent for memory cells[9]. Compared with naive cells, both memory subsets displayed increased sensitivity to stimulation by anti-CD3, both in the presence and in the absence of costimulation, although CCR7$^-$ cells were consistently more responsive (Fig. 4a). The capacity to stimulate IL-12 production was tested by co-culturing T cells with dendritic cells pulsed with different doses of the bacterial superantigen TSST. CCR7$^+$ memory cells efficiently stimulated IL-12 production by dendritic cells at both high and low doses of TSST, whereas naive T cells were much less effective and only stimulated IL-12 at the highest TSST dose (Fig. 4b). Thus, because of their lower triggering threshold and higher capacity to upregulate CD40L, CCR7$^+$ memory cells can function as potent activators of dendritic cells.

The above results indicated that two subsets of circulating memory T cells with different functional capacities can be discriminated by the expression of CCR7; therefore, we considered whether memory for antigens would be present in both subsets. As reported[16], proliferative responses to tetanus toxoid can not be detected in naive T cells; however, they were consistently found in both the CCR7$^+$ and CCR7$^-$ memory subsets, even ten years after vaccination (Fig. 5). Following a booster with tetanus toxoid, the proliferative responses increased in both subsets, indicating that their relative proportions are not affected by recent antigenic stimulation. In all cases, IFN-γ was produced by only the CCR7$^-$ memory cells. Comparable results were obtained by analysing the response to tetanus toxoid or hepatitis B surface antigen in five primed donors, showing that both memory subsets contain clonally expanded antigen-specific T cells, but these differ in their effector capacity. The presence of expanded antigen-specific memory cells in both subsets at different times after antigenic stimulation indicates that homeostatic mechanisms may maintain cells in both compartments[16,27,28].

What is the relationship between naive cells and the cells in the two memory subsets? When peripheral blood naive T cells were polyclonally stimulated, all cells became CD45R0$^+$ after 10 days (data not shown), but most of the cells retained CCR7 expression, whereas only a few acquired the capacity to produce IL-4 or IFN-γ (Fig. 6a–c). When the CCR7$^+$ and CCR7$^-$ cells were sorted and stimulated, IL-4, IL-5 and IFN-γ were found to be exclusively produced by the CCR7$^-$ cells (Fig. 6d). Thus, with respect to the parameters analysed, it appears that the same functional subsets of memory T cells that are detected *in vivo* can be generated by stimulation of naive cells in short-term culture.

When peripheral blood CCR7$^+$ memory T cells were sorted and stimulated under the same conditions, almost all the cells that were recovered after 10 days had lost CCR7 expression and had acquired the capacity to produce effector cytokines upon further stimulation (Fig. 6e–g), indicating that this subset is poised to generate effector cells. Finally, peripheral blood CCR7$^-$ memory cells, after stimulation and expansion, retained their CCR7$^-$ phenotype and effector function (Fig. 6h–j). This indicates that, at least *in vitro*, there may be a stepwise differentiation from naive T cells to CCR7$^+$ memory to CCR7$^-$ memory/effector T cells. This possibility is supported by analysis of the telomere length, which decreases as a function of cell division[29]. As shown in Fig. 6k, the length of telomeres in peripheral blood CD4 subsets decreased progressively from naive to memory

cells, but was consistently higher in the $CCR7^+$ than in the $CCR7^-$ subset, suggesting that the latter had undergone a larger number of divisions.

We have shown that immunological memory is displayed by distinct T-cell subsets: lymph-node-homing cells lacking inflammatory and cytotoxic function (which we define as central memory T cells, T_{CM}) and tissue-homing cells endowed with various effector functions (which we define as effector memory T cells, T_{EM}). These two subsets allow a division of labour among memory cells. On the one hand, T_{EM} cells represent a readily available pool of antigen-primed cells which can enter peripheral tissues to mediate inflammatory reactions or cytotoxicity, thus rapidly containing invasive pathogens. On the other hand, the newly described T_{CM} cells represent a clonally expanded antigen-primed population which travels to secondary lymphoid organs and, upon a secondary challenge, can efficiently stimulate dendritic cells, help B cells and generate a new wave of effector cells.

Our results indicate a precursor–product relationship between the two memory subsets. *In vitro* stimulation of naive T cells results in the generation of both T_{CM} and T_{EM} cells, whereas stimulation of T_{CM} cells results in their efficient differentiation to T_{EM} cells. Furthermore, antigen-specific T_{CM} and T_{EM} cells persist *in vivo* for up to ten years and their relative proportions do not change after a booster immunization. These data are consistent with a linear differentiation model in which naive T cells differentiate first to T_{CM} and then to T_{EM} cells, depending on the strength and duration of T-cell receptor stimulation and the presence or absence of polarizing cytokines[21]. Understanding the mechanisms that generate and maintain the two types of memory cells will help to manipulate immunological memory for vaccination and for adoptive immunotherapy. □

Methods

Sorting and FACS analysis

Peripheral blood mononuclear cells were stained with a rat monoclonal antibody (mAb) specific for CCR7 (3D12, IgG2a) followed by a fluorescein isothiocyanate (FITC)-labelled mouse anti-rat IgG2a mAb (PharMingen) or alternatively by a phycoerythrin (PE)-labelled goat anti-rat immunoglobulin polyclonal antiserum (Southern Biotechnology Associates). The 3D12 mAb completely inhibited migration of peripheral blood T cells in response to secondary lymphoid tissue chemokine (SLC) and EBI1-ligand chemokine (ELC) (R.F., unpublished data) and did not affect the response of T cells to mitogenic or antigenic stimulation (F.S., unpublished data). In addition, 3D12 stained all cell lines that expressed CCR7 messenger RNA, but did not stain CCR7 mRNA-negative cells. In some experiments, a mouse mAb specific for CCR7 (10H5, IgG3; produced by L. Wu, LeukoSite) was used with comparable results. The following PE-, PC5- or APC-labelled mouse mAbs were used in different combinations: anti-CD45RA (ALB11, IgG1); anti-CD45R0 (UCHL1, IgG2a); anti-CD3 (UCHT1, IgG1); anti-CD4 (13B8.2, IgG1); anti-CD8 (B9.11, IgG1); anti-CD11a (25.3, IgG1); anti-CD11b (Bear1, IgG1); anti-CD18 (7E4, IgG1); anti-CD49d (HP2/1, IgG1); anti-CD49e (SAM1, IgG2b); anti-CD29 (K20, IgG2a); anti-CD103 (2G5, IgG2a); anti-CD69 (TP1.55, IgG2b); anti-CD25 (B1.49, IgG2a); anti HLA-DR (B8.12, IgG2b); anti-CD40L (TRAP-1, IgG1) (all from Immunotech); and anti-CLA (HECA-205, rat IgG1; PharMingen). Staining for chemokine receptors was carried out using the following mouse mAbs (all produced at LeukoSite): anti-CCR1 (2D4, IgG1); anti-CCR3 (7B11, IgG2a); anti-CCR4 (1G1, IgG1); anti-CCR5 (2D7, IgG2a); anti-CCR6 (11A9, IgG1); anti-CXCR3 (1C6, IgG1); and anti-CXCR4 (12G5, IgG2a). Cells were sorted using a fluorescence-activated cell sorter (FACS Vantage) and analysed on a FACScalibur (Becton Dickinson Systems). Sorted cells were immobilized on poly-L-lysine coated slides, fixed in 2% paraformaldehyde and permeabilized in 0.1% Triton-X100 before intracellular staining with an anti-perforin mAb (2δ4, IgG2b; PharMingen), followed by FITC-labelled goat anti-mouse immunoglobulin and propidium iodide to visualize the nuclei by confocal microscopy. The length of telomeres was determined using a Teloquant kit (PharMingen).

Cytokine detection

T cells were stimulated with 10 μg ml^{-1} anti-CD3 antibody (TR66, IgG1) and 10^{-7} M phorbol 12-myristate 13-acetate (PMA; Sigma). Cytokine production was measured in the 24-h culture supernatants by ELISA using matched pairs of antibodies specific for IL-2, IL-4, IL-5, IFN-γ (PharMingen). For cytokine detection at the single-cell level, T cells were stimulated with 10^{-7} M PMA and 1 μg ml^{-1} ionomycin for 4 h, or with autologous dendritic cells pulsed with 100 ng ml^{-1} TSST for 7 h in 10 μg ml^{-1} brefeldin A. Cells were fixed and permeabilized with PBS containing FCS (2%) and saponin (0.5%) and stained with FITC-labelled anti-IFN-γ (IgG1) and PE-labelled anti-IL-4 (IgG2b) or PE-labelled anti-CD69 mAbs.

Cell cultures

Sorted cells were stimulated with plastic-bound anti-CD3 (TR66) and anti-CD28 (CD28.1, IgG1; provided by D. Olive) in RPMI 1640 medium containing 2 mM L-glutamine, 1% non-essential amino acids, 1% sodium pyruvate, 50 μg ml^{-1} kanamycin, (complete medium; Gibco BRL) and 10% FCS (HyClone Laboratories). The cells were expanded with 500 U ml^{-1} IL-2. Monocytes were isolated using magnetic beads coated with anti-CD14 mAb (Miltenyi), irradiated (3,000 rad), pulsed with 5 μg ml^{-1} TT and cultured with different numbers of T cells. IFN-γ was measured by ELISA in the 24-h culture supernatant. ^{3}H-thymidine incorporation was measured on day five. Immature dendritic cells were produced by culturing peripheral blood $CD14^+$ monocytes with GM-CSF + IL-4 for six days. The cells were pulsed with different concentrations of TSST and cultured with graded numbers of T cells. IL-12 p70 was measured by ELISA (PharMingen) in the 24-h culture supernatant.

Received 6 May; accepted 4 August 1999.

1. Butcher, E. C. & Picker, L. J. Lymphocyte homing and homeostasis. *Science* **272,** 60–66 (1996).
2. Banchereau, J. & Steinman, R. M. Dendritic cells and the control of immunity. *Nature* **392,** 245–252 (1998).
3. MacLennan, I. C. *et al.* The changing preference of T and B cells for partners as T-dependent antibody responses develop. *Immunol. Rev.* **156,** 53–66 (1997).
4. Garside, P. *et al.* Visualization of specific B and T lymphocyte interactions in the lymph node. *Science* **281,** 96–99 (1998).
5. Mackay, C. R. Homing of naive, memory and effector lymphocytes. *Curr. Opin. Immunol.* **5,** 423–427 (1993).
6. Austrup, F. *et al.* P- and E-selectin mediate recruitment of T-helper-1 but not T-helper-2 cells into inflamed tissues. *Nature* **385,** 81–83 (1997).
7. Ahmed, R. & Gray, D. Immunological memory and protective immunity: understanding their relation. *Science* **272,** 54–60 (1996).
8. Zinkernagel, R. M. *et al.* On immunological memory. *Annu. Rev. Immunol.* **14**, 333–367 (1996).
9. Dutton, R. W., Bradley, L. M. & Swain, S. L. T cell memory. *Annu. Rev. Immunol.* **16,** 201–223 (1998).
10. Gunn, M. D. *et al.* A chemokine expressed in lymphoid high endothelial venules promotes the adhesion and chemotaxis of naive T lymphocytes. *Proc. Natl Acad. Sci USA* **95,** 258–263 (1998).
11. Campbell, J. J. *et al.* Chemokines and the arrest of lymphocytes rolling under flow conditions. *Science* **279,** 381–384 (1998).
12. Campbell, J. J. *et al.* 6-C-kine (SLC), a lymphocyte adhesion-triggering chemokine expressed by high endothelium, is an agonist for the MIP-3β receptor CCR7. *J. Cell Biol.* **141,** 1053–1059 (1998).
13. Mackay, C. R., Marston, W. L. & Dudler, L. Naive and memory T cells show distinct pathways of lymphocyte recirculation. *J. Exp. Med.* **171,** 801–817 (1990).
14. Baggiolini, M. Chemokines and leukocyte traffic. *Nature* **392,** 565–568 (1998).
15. Gunn, M. D. *et al.* Mice lacing expression of secondary lymphoid organ chemokine have defects in lymphocyte homing and dendritic cell localization. *J. Exp. Med.* **189,** 451–460 (1999).
16. Michie, C. A., McLean, A., Alcock, C. & Beverley, P. C. Lifespan of human lymphocyte subsets defined by CD45 isoforms. *Nature* **360,** 264–265 (1992).
17. Baron, J. L., Madri, J. A., Ruddle, N. H., Hashim, G. & Janeway, C. A. Jr Surface expression of alpha 4 integrin by CD4 T cells is required for their entry into brain parenchyma. *J. Exp. Med.* **177,** 57–68 (1993).
18. Wu, L. *et al.* CCR5 levels and expression pattern correlate with infectability by macrophage-tropic HIV-1, *in vitro*. *J. Exp. Med.* **185,** 1681–1691 (1997).
19. Sallusto, F., Mackay, C. R. & Lanzavecchia, A. Selective expression of the eotaxin receptor CCR3 by human T helper 2 cells. *Science* **277,** 2005–2007 (1997).
20. Tang, H. L. & Cyster, J. G. Chemokine up-regulation and activated T cell attraction by maturing dendritic cells. *Science* **284,** 819–822 (1999).
21. Sallusto, F., Lenig, D., Mackay, C. R. & Lanzavecchia, A. Flexible programs of chemokine receptor expression on human polarized T helper 1 and 2 lymphocytes. *J. Exp. Med.* **187,** 875–883 (1998).
22. Grewal, I. S. & Flavell, R. A. CD40 and CD154 in cell-mediated immunity. *Annu. Rev. Immunol.* **16,** 111–135 (1998).
23. Abbas, A. K., Murphy, K. M. & Sher, A. Functional diversity of helper T lymphocytes. *Nature* **383,** 787–793 (1996).
24. Kagi, D., Ledermann, B., Burki, K., Zinkernagel, R. M. & Hengartner, H. Molecular mechanisms of lymphocyte-mediated cytotoxicity and their role in immunological protection and pathogenesis *in vivo*. *Annu. Rev. Immunol.* **14,** 207–232 (1996).
25. Casamayor-Palleja, M., Khan, M. & MacLennan, I. C. A subset of CD4+ memory T cells contains preformed CD40 ligand that is rapidly but transiently expressed on their surface after activation through the T cell receptor complex. *J. Exp. Med.* **181,** 1293–1301 (1995).
26. Hamann, D. *et al.* Phenotypic and functional separation of memory and effector human CD8+ T cells. *J. Exp. Med.* **186,** 1407–1418 (1997).
27. Sprent, J., Tough, D. F. & Sun, S. Factors controlling the turnover of T memory cells. *Immunol. Rev.* **156,** 79–85 (1997).
28. Tanchot, C. & Rocha, B. The organization of mature T-cell pools. *Immunol. Today* **19,** 575–579 (1998).
29. Weng, N. P., Hathcock, K. S. & Hodes, R. J. Regulation of telomere length and telomerase in T and B cells: a mechanism for maintaining replicative potential. *Immunity* **9,** 151–157 (1998).

Acknowledgements

We thank K. Hannestad and K. Karjalainen for critical reading; J. C. Howard for his help as 'wordsmith'; M. Dessing and A. Pickert for cell sorting; A. Hoy for help in the initial experiments; LeukoSite Inc., Cambridge, Massachusetts for providing antibodies to chemokine receptors; and L. Wu for providing the CCR7 and CCR4 antibodies before publication. The Basel Institute for Immunology was founded and is supported by F. Hoffmann-La Roche Ltd, Basel, Switzerland.

Correspondence should be addressed to F.S. (e-mail: sallusto@bii.ch).